Microfluidic assisted synthesis of multi-functional polycaprolactone microcapsules: incorporation of CdTe quantum dots, Fe_3O_4 superparamagnetic nanoparticles and tamoxifen anticancer drugs†

C.-H. Yang,*[a] K.-S. Huang,[b] Y.-S. Lin,[c] K. Lu,[d] C.-C. Tzeng,[e] E.-C. Wang,[e] C.-H. Lin,[f] W.-Y. Hsu[a] and J.-Y. Chang[g]

Received 27th August 2008, Accepted 24th November 2008
First published as an Advance Article on the web 19th December 2008
DOI: 10.1039/b814952f

This paper demonstrates a proof-of-concept approach for encapsulating the anticancer drug tamoxifen, Fe_3O_4 nanoparticles (NPs) and CdTe quantum dots (QDs) into size-controlled polycaprolactone (PCL) microcapsules utilizing microfluidic emulsification, which combined magnetic targeting, fluorescence imaging and drug controlled release properties into one drug delivery system. Cross-linking the composite PCL microcapsules with poly(vinyl alcohol) (PVA) tailored their size, morphology, optical and magnetic properties and drug release behaviors. The flow conditions of the two immiscible solutions were adjusted in order to successfully generate various sizes of polymer droplets. The result showed superparamagnetic and fluorescent properties, and was used as a controlled drug release vehicle. The composite magnetic and fluorescent PCL microcapsules are potential candidates for a smart drug delivery system.

1 Introduction

The unique and tunable optical, magnetic, and chemical features of inorganic components such as magnetic nanoparticles (NPs) and quantum dots (QDs) are increasingly finding use in the field of medicine. Magnetic NPs have been widely studied because of their potential application in the biomedical field, such as biomolecular separation and magnetic resonance imaging.[1] They also offer exciting new opportunities for developing effective drug delivery systems.[2] An external localized magnetic field gradient may be applied to a chosen site to attract drug-loaded magnetic nanoparticles *via* the blood circulation system, thereby reducing the side effects of conventional chemotherapy by reducing the systemic distribution of drugs as well as lowering the doses of the cytotoxic compounds. QDs have gained increasing attention in technological applications and fundamental studies.[3] Their size-controlled fluorescence properties, their high fluorescence quantum yields, and their stability against photobleaching make QDs suitable as light-emitting materials for biolabeling applications.

In the past decades, biodegradable and biocompatible polymers have received significant attention because they are environmentally friendly and they are extensively used in biomedical applications. Polycaprolactone (PCL), a semi-crystalline linear resorbable aliphatic polyester, is subject to biodegradation because of the susceptibility of its aliphatic ester linkage to hydrolysis, and it can be used as the matrix for bone substitutes, scaffolds, and drug carriers for controlled release.[4] Extensive *in vitro* and *in vivo* biocompatibility and efficacy studies have been carried out, resulting in US Food and Drug Administration (FDA) approval of a number of medical and drug delivery devices. For drug delivery vehicles, a uniform size of the microcapsules is crucial, because the drug release kinetics can be manipulated, making it easier to formulate more sophisticated systems.

Microfluidic devices are ideal for obtaining uniform-size microcapsules since they have the advantage of continuous, reproducible and scalable production.[5] Microfluidic systems are becoming increasingly useful for a range of analytical and chemical processes, especially for producing droplets with highly uniform size, which are being developed by a number of research groups.[6] However, less attention has been paid to acquiring microcapsules containing both anticancer drugs and functional nanomaterials.[7] In this work, a novel drug delivery system has been developed, based on magnetic and fluorescent multifunctional PCL microcapsules, combining magnetic targeting, fluorescent imaging and drug controlled release properties into one drug delivery system.

2 Results and discussion

The fabrication process of a polydimethylsiloxane (PDMS) microfluidic platform is shown in Fig. 1a. The microfluidic chip consists of three inlet ports, an outlet port, a cross-junction

[a]*Dept. of Biological Science & Technology, I-Shou University, Taiwan. E-mail: chyang@isu.edu.tw; Fax: +886-7-615-1959; Tel: +886-7-615-1100 ext. 7312*
[b]*Dept. of Biomedical Engineering, I-Shou University, Taiwan*
[c]*Instrument Technology Research Center, National Applied Research Laboratories, Taiwan*
[d]*Dept. of Physical Therapy, I-Shou University, Taiwan*
[e]*Faculty of Medicinal and Applied Chemistry, Kaohsiung Medical University, Taiwan*
[f]*Dept. of Mechanical and Electro-Mechanical Engineering, National Sun Yat-Sen University, Taiwan*
[g]*Nanopowder and Thin Film Technology Center, Industrial Technology Research Institute, Taiwan*
† Electronic supplementary information (ESI) available: Experimental details. See DOI: 10.1039/b814952f

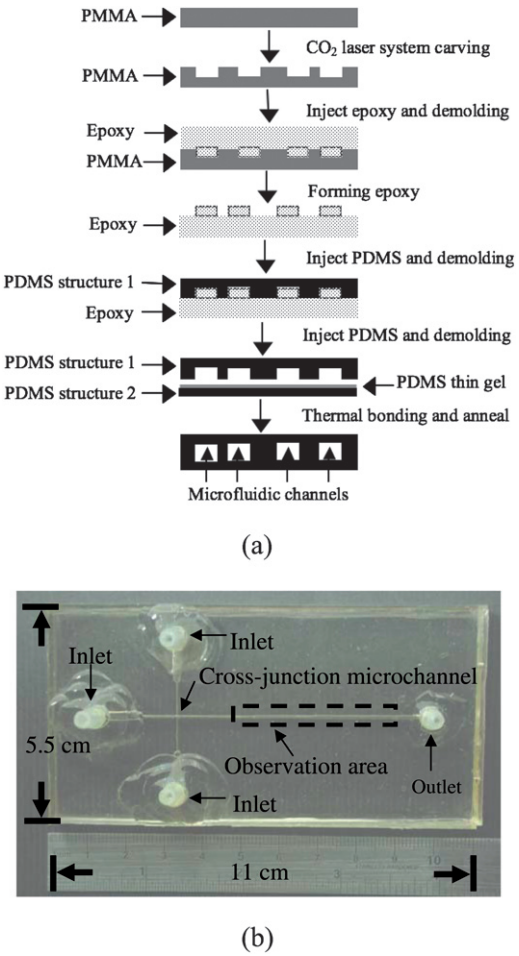

Fig. 1 (a) Scheme depicting the fabrication process of a microfluidic chip (side view). (b) Photograph of a microfluidic device illustrating the channel layout and the connection inlet and outlet (top view). (PMMA: polymethyl methacrylate; PDMS: polydimethylsiloxane).

channel and an observation chamber (Fig. 1b). Fig. 2 shows the transmission electron microscope (TEM) images which reveal the size distribution of Fe_3O_4 NPs and CdTe QDs with an average size of 5.5 ± 1.0 nm and 4.5 ± 0.5 nm, respectively. High resolution TEM (HRTEM) images of Fe_3O_4 NPs and CdTe QDs have been improved to demonstrate their lattice fringes, and are shown in the inset.[8]

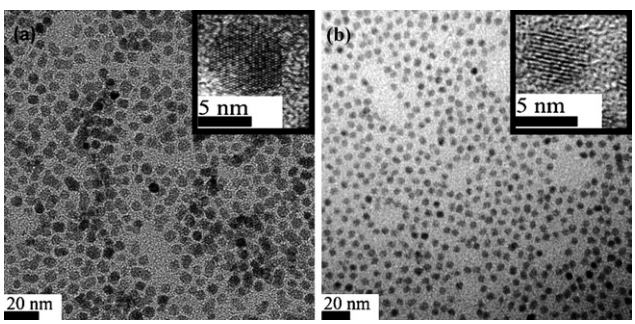

Fig. 2 Transmission electron microscope (TEM) micrographs of (a) Fe_3O_4 nanoparticles (NPs) (inset: the corresponding high resolution transmission electron microscope (HRTEM) image), and (b) CdTe quantum dots (QDs) deposited from dispersions in chloroform (inset: the corresponding HRTEM image).

The microfluidic emulsification method is based on the competition between two opposite processes, drop breakage and drop–drop coalescence in the bulk solution. Both processes are

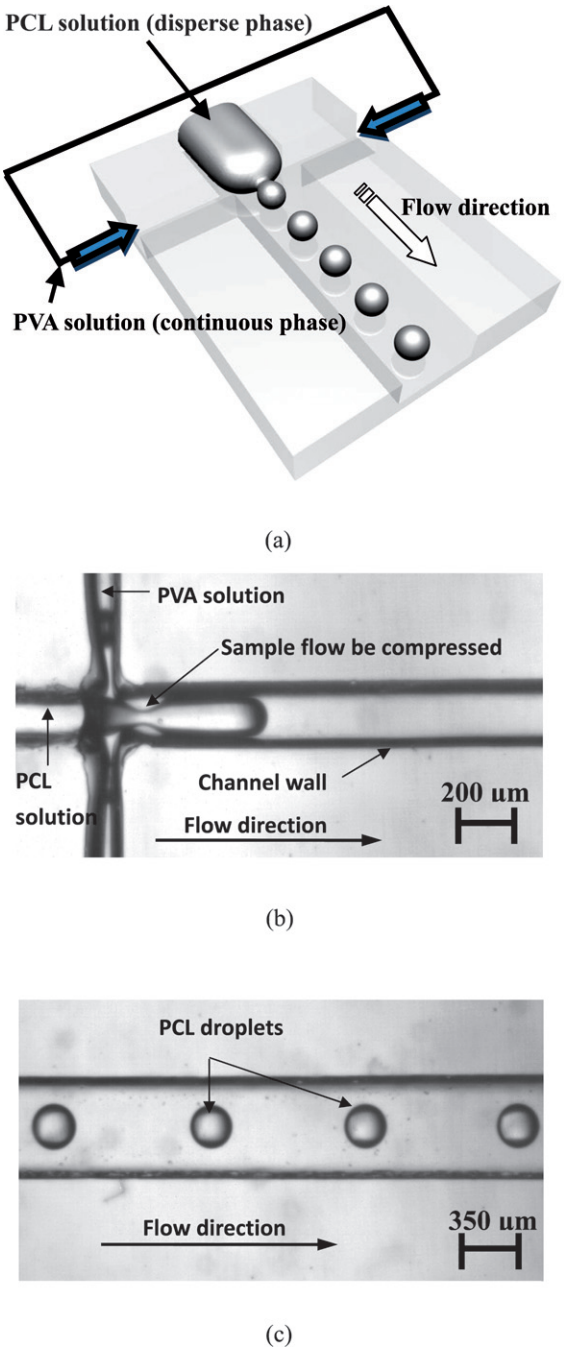

Fig. 3 (a) Schematic drawing in top view of the formation of droplets in a cross-junction microchannel (not to scale). By applying microfluidics to exert control over the shear focusing force, a large set of uniform self-assembling PCL droplets can be obtained. (b) Photograph at the cross-junction microchannel: a PCL droplet is generated (scale bar is 200 μm). (c) Photograph at the observation chamber: PCL droplets encapsulating the anticancer drug tamoxifen, Fe_3O_4 NPs and CdTe QDs (scale bar is 350 μm). (PCL: polycaprolactone; PVA: poly(vinyl alcohol)).

Table 1 The relationships among the average droplet diameter, the relative sheath/sample flow velocities at various driving frequencies, and the entrapped composition of per PCL capsule.

Flow rate of dispersed phase (mL/min)	Flow rate of continuous phase (mL/min)	Droplet		Concentration		
		Average size (μm)	RSD[a] (%)	CdTe (mole)	Fe_3O_4 (mole)	Tamoxifen (mole)
0.02	0.8	319	3.2	4.10×10^{-12}	1.92×10^{-11}	1.11×10^{-11}
	0.9	315	0.2	3.95×10^{-12}	1.85×10^{-11}	1.06×10^{-11}
	1	274	1.3	2.60×10^{-12}	1.22×10^{-11}	7.01×10^{-12}
0.03	0.8	353	0.1	5.57×10^{-12}	2.61×10^{-11}	1.50×10^{-11}
	0.9	346	0.1	5.22×10^{-12}	2.45×10^{-11}	1.41×10^{-11}
	1	323	0.3	4.24×10^{-12}	1.99×10^{-11}	1.14×10^{-11}
0.04	0.8	361	0.1	5.94×10^{-12}	2.79×10^{-11}	1.60×10^{-11}
	0.9	346	0.3	5.23×10^{-12}	2.45×10^{-11}	1.41×10^{-11}
	1	338	0.1	4.88×10^{-12}	2.29×10^{-11}	1.31×10^{-11}
0.05	0.8	438	0.1	1.06×10^{-11}	4.97×10^{-11}	2.85×10^{-11}
	0.9	400	0.2	8.06×10^{-12}	3.78×10^{-11}	2.17×10^{-11}
	1	378	0.1	6.83×10^{-12}	3.21×10^{-11}	1.84×10^{-11}

[a] RSD: relative standard deviation.

promoted by the intensive stirring of the oil–water mixture inside the emulsification chamber and result in considerable polydispersity of size distribution. Fig. 3a shows the top view of a microfluidic chip with a cross-junction. In this study, oil-in-water (o/w) emulsions are formed by shearing one liquid into a second immiscible one, and regular-sized emulsions are then generated in the microfluidic platform. As shown in Fig. 3b, two different fluids were supplied simultaneously to the microfluidic system: the PCL solution (dispersed phase which composed of PCL, tamoxifen, CdTe QDs and Fe_3O_4 NPs in chloroform) was supplied from the central inlet channel, and the poly(vinyl alcohol) (PVA) solution (continuous phase) was supplied from two side channels of the microfluidic device. PVA was utilized as a hydrophilic additive to improve the hydrophilicity of the PCL microspheres. The regular emulsion droplets composed of tamoxifen, CdTe QDs and Fe_3O_4 NPs were detected in the observation zone (Fig. 3c). The broadened channel (600 μm in width, downstream of the cross channel) at the observation chamber was designed to slow down the flow and to enhance the observation.

The size of the droplet can be easily modulated by adjusting the flow condition in the microchannels. Table 1 illustrates the relationships between the flow speed (average velocity) of the phases and the droplet size. For a given 1 mL/min of the continuous phase flow, the droplet size increases as the average velocity of the dispersed phase (PCL solution) flow increases. For a given 0.04 mL/min of the dispersed phase flow, the droplet size decreases as the average velocity of the continuous phase increases. In each flow condition, the droplets have a relative standard deviation (RSD) of less than 4%. In addition, the proposed microfluidic device shows a good linear correlation between droplet size and flow rate. This is very important for its practical application in quantitative analysis.

After the microfluidic synthesis of the PCL droplets, the schematic illustration of the PCL microcapsules formation was carried out using the solvent evaporation process (Fig. 4). During this process, the removal of chloroform was accompanied by shrinkage of the microcapsules because of the progressive cross-linking of the PCL matrix. Fig. 5a and 5c are typical optical microscopy images of PCL microdroplets composed of tamoxifen, CdTe QDs and Fe_3O_4 NPs. These microdroplets form a hexagonal closely packed structure typical for a microgel, and exhibit excellent size uniformity. After removal of the chloroform through evaporation, the PCL microcapsules (Fig. 5b and 5d) are allowed to shrink further and form smaller and denser matrices. The shrinkage (mean 16%) of the PCL

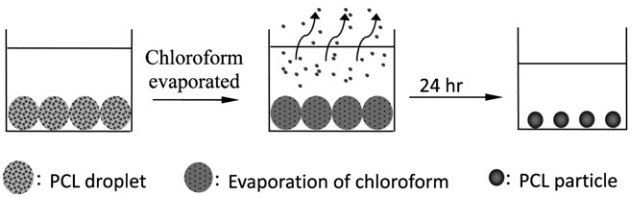

Fig. 4 Schematic illustrations of the PCL microcapsules formation in the reservoir.

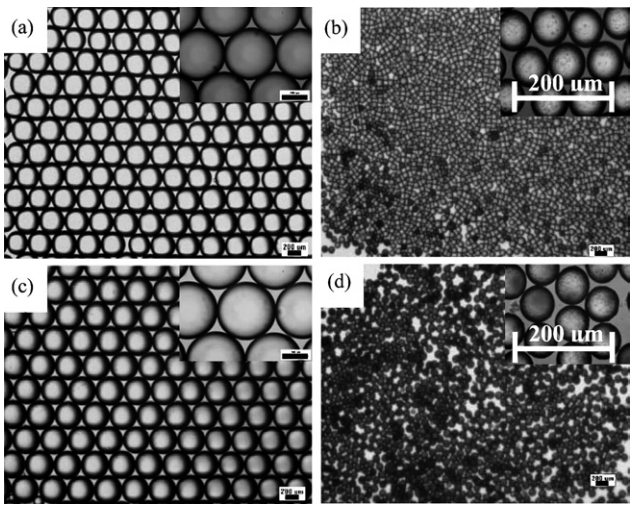

Fig. 5 Microscope images of various uniform PCL microdroplets (a) and (c), and PCL microcapsules (b) and (d). (b) is the photo image after evaporation of chloroform in (a). (d) is the photo image after evaporation of chloroform in (b). (All scale bars are 200 μm).

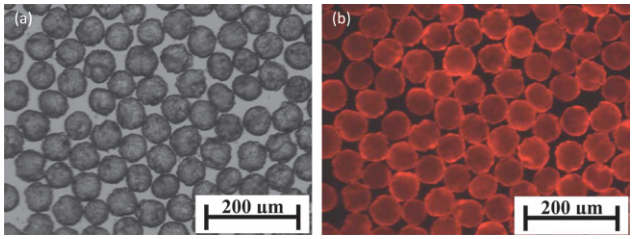

Fig. 6 The photo images of the functional PCL microcapsules composed of tamoxifen, CdTe QDs and Fe_3O_4 NPs are observed in the collection reservoir. (a) Bright-field optical and (b) fluorescent microscope images taken through a 10× microscope objective.

microcapsules is believed to be due to the removal of the chloroform content during the evaporation procedure.

After exciting at 350 nm (frequency tripled Surelite I-10 Nd:YAG laser emission), the imaging shows that the fluorescence signals are across the internal areas of each PCL microcapsule, demonstrating the encapsulation of QDs in the microcapsule's interior (Fig. 6b). The particle size of Fig. 6 is 67 ± 6.2 μm in diameter. A variation in particle size (after evaporation of the chloroform) of <10% was observed in the proposed system, which is larger than the variation in droplets (before evaporation of the chloroform, <4%). In addition, a general reduction in the spherical quality of the particles was observed. For the CdTe QDs, the extinction spectrum remains nearly unchanged before and after embedding them in PCL microspheres. This demonstrates that each microsphere entraps numerous QDs in a protective PCL matrix.

The PCL microcapsules of 50–200 μm with narrow size distribution are useful carriers for drug release systems since they provide transportation for various drug forms. Like most low molecular weight drugs, tamoxifen has a short blood circulation time, which reduces tumor uptake and intracellular DNA binding. The encapsulation of tamoxifen in PCL microcapsules provides micro-environmental protection, benefits from prolonged blood circulation and reduces dose-limiting toxicities. It was expected that in this microfluidic system the entire amount of tamoxifen could be entrapped in the PCL droplets without partitioning it into the immiscible phase, because o/w emulsions are formed by shearing one liquid into a second immiscible one. Fig. 7 shows the tamoxifen release curves of the PCL microcapsules (60 μm). About 78% of the entrapped drug was released in the first 24 h, and 100% was released within 2 days. The tamoxifen release profile of the PCL microcapsules expresses two stages: burst release (17% of the tamoxifen encapsulated) and sequential slow release. The burst release may be due to some tamoxifen imbedded in the PCL microcapsule surface or in the incomplete solidified surface of the microcapsule. According to the review by Huang and Brazel,[9] diffusion and migration of tamoxifen may occur during the drying process as chloroform moves to the gel surface and evaporates. Drugs may diffuse by convection with water, leaving an uneven drug distribution across the gel, with higher concentrations at the surface. The initial burst release can provide a loading dose for tamoxifen rapidly reaching the therapeutic window. The mechanism of this slow release may involve: (1) biodegradation of PCL, (2) PCL microcapsules swelling, and (3) diffusion of tamoxifen molecules

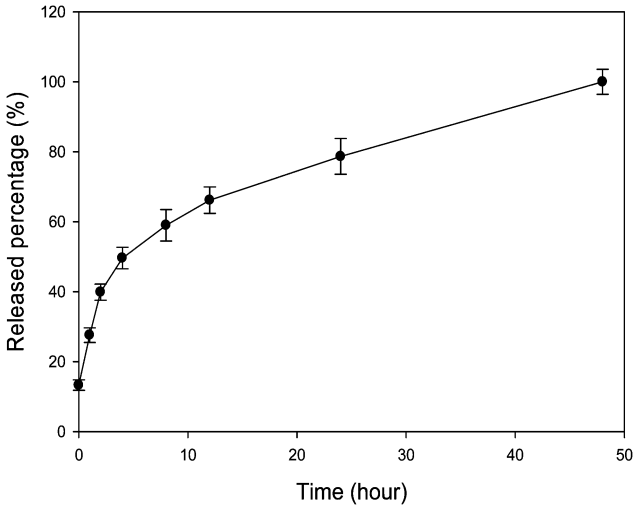

Fig. 7 *In vitro* release profile of tamoxifen from the PCL microcapsules. Data represent mean ± SD, $n = 3$.

through the swollen PCL microcapsule. The results of the drug release pattern indicate that the release rate of the tamoxifen achieved the objective of the sustained release dosing protocol for clinical use.

To assess the magnetic properties of the functional PCL microcapsules, we investigated their response when subjected to an external magnetic field. The magnetic properties of the functional PCL microcapsules were recorded using a superconducting quantum interference device (SQUID) magnetometer with fields up to 70 KOe. Hysteresis loops of the samples were registered at temperatures of 10 and 300 K (Fig. 8a). The saturation magnetization value of functional PCL microcapsules is 42 and 33 emu/g at 10 K and 300 K, respectively. The zero coercivity and the reversible hysteresis behavior indicate the superparamagnetic nature of the functional PCL microcapsules. The magnetic separability of these functional PCL microcapsules was tested in ethanol by placing a magnet near the glass bottle. The black particles were attracted toward the magnet within 60 s (Fig. 8b), clearly demonstrating that the functional PCL microcapsules possess magnetic properties. This provides an easy and

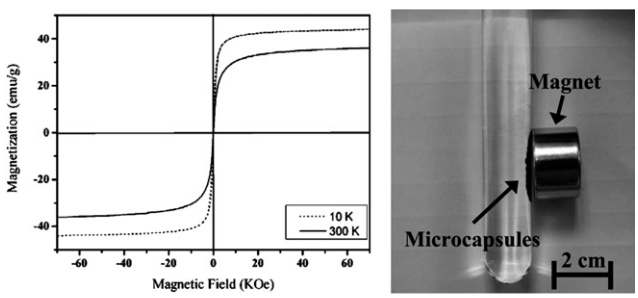

Fig. 8 (a) Magnetic measurements of the triple-functional PCL microcapsules showing the magnetization–applied magnetic field and (b) a photograph of the microcapsules attached to the side of the vial by an external magnetic field.

efficient way to separate the functional PCL microcapsules from a sol, or suspension system, and to carry drugs to targeted locations under an external magnetic field.

3 Conclusion

We successfully proposed a facile and one-pot method for producing functional PCL microcapsules, entrapping anticancer drug, fluorescent and superparamagnetic NPs *via* the o/w emulsion system in a microchannel cross-junction. In this microfluidic system, the entire amount of the anticancer drug and various nanoparticles can be entrapped in the PCL phase without partitioning into the immiscible phase caused when o/w emulsions are formed by shearing one liquid into a second immiscible one. The size-controllable PCL microcapsule can be created from 270 μm to 440 μm in diameter with a size distribution (within ±4%) by altering the ratio of the flow rate. A production rate of on average 300 mg/hour of PCL microcapsules can be obtained by the proposed microfluidic system. For the purpose of mass production, Nisisako and Torii reported a co-flow module microfluidic device for the mass production of particles (~ 0.3 kg/hour).[10] In our future work we will attempt to employ a massive parallelized microfluidic device to prepare functional PCL microcapsules to prove the practicality of our process. As a consequence of these distinct properties, a combination of fluorescent and magnetic properties in one PCL microcapsule enables simultaneous biolabeling and target-drug delivery. In the future our method can be used to fabricate various size-controlled composite microparticles to act as a smart drug delivery system.

Acknowledgements

This work was financially supported by a grant from the National Science Council of Taiwan, R.O.C. (97-2320-B-214-002-MY3 and 97-2314-B-214-004).

References

1 (*a*) J. Park, K. An, Y. Hwang, J.-G. Park, H.-J. Noh, J.-Y. Kim, J.-H. Park, N.-M. Hwang and T. Hyeon, *Nat. Mater.*, 2004, **3**, 891–895; (*b*) Y.-M. Huh, Y.-w. Jun, H.-T. Song, S. Kim, J.-s. Choi, J.-H. Lee, S. Yoon, K.-S. Kim, J.-S. Shin, J.-S. Suh and J. Cheon, *J. Am. Chem. Soc.*, 2005, **127**, 12387–12391.
2 (*a*) J.-M. Nam, C. S. Thaxton and C. A. Mirkin, *Science*, 2003, **301**, 1884–1886; (*b*) I. Willner and E. Katz, *Angew. Chem., Int. Ed.*, 2003, **42**, 4576–4588.
3 (*a*) M. Bruchez, Jr., M. Moronne, P. Gin, S. Weiss and A. P. Alivisatos, *Science*, 1998, **281**, 2013–2016; (*b*) W. C. W. Chan and S. Nie, *Science*, 1998, **281**, 2016–2018; (*c*) X. Michalet, F. F. Pinaud, L. A. Bentolila, J. M. Tsay, S. Doose, J. J. Li, G. Sundaresan, A. M. Wu, S. S. Gambhir and S. Weiss, *Science*, 2005, **307**, 538–544; (*d*) I. L. Medinitz, H. T. Uyeda, E. R. Goldman and H. Mattoussi, *Nat. Mater.*, 2005, **4**, 435–446.
4 (*a*) R. S. Bezwada, D. D. Jamiolkowski, I.-Y. Lee, V. Agarwal, J. Persivale, S. Trenka-Benthin, M. Erneta, J. Suryadevara, A. Yang and S. Liu, *Biomaterials*, 1995, **16**, 1141–1148; (*b*) J. John, J. Tang, Z. Yang and M. Bhattacharya, *J. Polym. Sci. Part A: Polym. Chem.*, 1997, **35**, 1139–1148; (*c*) G. Gorrasi, M. Tortora, V. Vittoria, E. Pollet, B. Lepoittevin, M. Alexandre and P. Dubois, *Polymer*, 2003, **44**, 2271–2279; (*d*) V. R. Sinha, K. Bansal, R. Kaushik, R. Kumria and A. Trehan, *Int. J. Pharm.*, 2004, **278**, 1–23.
5 (*a*) M. U. Kopp, A. J. de Mello and A. Manz, *Science*, 1998, **280**, 1046–1048; (*b*) T. Thorsen, R. W. Roberts, F. H. Arnold and S. R. Quake, *Phys. Rev. Lett.*, 2001, **86**, 4163–4166; (*c*) B. H. Weigl, R. L. Bardell and C. R. Cabrera, *Adv. Drug Deliv. Rev.*, 2003, **55**, 349–377; (*d*) G. M. Whitesides, *Nature*, 2006, **442**, 368–373.
6 (*a*) S. Sugiura, M. Nakajima, S. Iwamoto and M. Seki, *Langmuir*, 2001, **17**, 5562–5566; (*b*) J. Kameoka, R. Orth, B. Ilic, D. Czaplewski, T. Wachs and H. G. Craighead, *Anal. Chem.*, 2002, **74**, 5897–5901; (*c*) M. Tokeshi, T. Minagawa, K. Uchiyama, A. Hibara, K. Sato, H. Hisamoto and T. Kitamori, *Anal. Chem.*, 2002, **74**, 1565–1571; (*d*) T. Nisisako, T. Torii and T. Higuchi, *Lab Chip*, 2002, **2**, 24–26; (*e*) S. L. Anna, N. Bontoux and H. A. Stone, *Appl. Phys. Lett.*, 2003, **82**, 364–366; (*f*) K. Martin, T. Henkel, V. Baier, A. Grodrian, T. Schön, M. Roth, J. M. Köhler and J. Metze, *Lab Chip*, 2003, **3**, 202–207; (*g*) J. D. Tice, H. Song, A. D. Lyon and R. F. Ismagilov, *Langmuir*, 2003, **19**, 9127–9133; (*h*) T. Vilkner, D. Janasek and A. Manz, *Anal. Chem.*, 2004, **76**, 3373–3386; (*i*) S. Okushima, T. Nisisako, T. Torii and T. Higuchi, *Langmuir*, 2004, **20**, 9905–9908; (*j*) Z. Nie, S. Xu, M. Seo, P. C. Lewis and E. Kumacheva, *J. Am. Chem. Soc.*, 2005, **127**, 8058–8063; (*k*) T. Nisisako, T. Torii, T. Takahashi and Y. Takizawa, *Adv. Mater.*, 2006, **18**, 1152–1156; (*l*) K.-S. Huang, T.-H. Lai and Y.-C. Lin, *Lab Chip*, 2006, **6**, 954–957; (*m*) P. Garstecki, M. J. Fuerstman, H. A. Stone and G. M. Whitesides, *Lab Chip*, 2006, **6**, 437–446; (*n*) W.-H. Tan and S. Takeuchi, *Adv. Mater.*, 2007, **19**, 2696–2701; (*o*) S. Sugiura, T. Oda, Y. Aoyagi, M. Satake, N. Ohkohchi and M. Nakajima, *Lab Chip*, 2008, **8**, 1255–1257; (*p*) S.-H. Kim, S.-J. Jeon, G.-R. Yi, C.-J. Heo, J. H. Choi and S.-M. Yang, *Adv. Mater.*, 2008, **20**, 1649–1655; (*q*) S. Abraham, Y. H. Park, J. K. Lee, C.-S. Ha and I. Kim, *Adv. Mater.*, 2008, **20**, 2177–2182; (*r*) J. Wan, A. Bick, M. Sullivan and H. A. Stone, *Adv. Mater.*, 2008, **20**, 3314–3318; (*s*) C.-H. Yang, Y.-S. Lin, K.-S. Huang, Y.-C. Huang, E.-C. Wang, J.-Y. Jhong and C.-Y. Kuo, *Lab Chip*, 2009, **9**, 145–150.
7 (*a*) H. Becker and L. E. Locascio, *Talanta*, 2002, **56**, 267–287; (*b*) D. T. Eddington and D. J. Beebe, *Adv. Drug Deliv. Rev.*, 2004, **56**, 199–210; (*c*) P. Garstecki, H. A. Stone and G. M. Whitesides, *Phys. Rev. Lett.*, 2005, **94**, 164501; (*d*) H. Song, D. L. Chen and R. F. Ismagilov, *Angew. Chem., Int. Ed.*, 2006, **45**, 7336–7356; (*e*) F. X. Gu, R. Karnik, A. Z. Wang, F. Alexis, E. Levy-Nissenbaum, S. Hong, R. S. Langer and O. C. Farokhzad, *Nano Today*, 2007, **2**, 14–21; (*f*) L. Kang, B. G. Chung, R. Langer and A. Khademhosseini, *Drug Discov. Today*, 2008, **13**, 1–13; (*g*) S.-Y. Teh, R. Lin, L.-H. Hung and A. P. Lee, *Lab Chip*, 2008, **8**, 198–220.
8 (*a*) S. Sun and H. Zeng, *J. Am. Chem. Soc.*, 2002, **124**, 8204–8205; (*b*) W. W. Yu and X. Peng, *Angew. Chem., Int. Ed.*, 2002, **41**, 2368–2371.
9 X. Huang and C. S. Brazel, *J. Control. Release.*, 2001, **73**, 121–136.
10 T. Nisisako and T. Torii, *Lab Chip*, 2008, **8**, 287–293.